

Enabling Efficient and Flexible Interpretability of Data-driven Anomaly Detection in Industrial Processes with AcME-AD

Valentina Zaccaria¹, Chiara Masiero², David Dandolo², Gian Antonio Susto¹

¹Department of Information Engineering, University of Padova, ²Statwolf Data Science Srl

Abstract—While Machine Learning has become crucial for Industry 4.0, its opaque nature hinders trust and impedes the transformation of valuable insights into actionable decision, a challenge exacerbated in the evolving Industry 5.0 with its human-centric focus. This paper addresses this need by testing the applicability of AcME-AD in industrial settings. This recently developed framework facilitates fast and user-friendly explanations for anomaly detection. AcME-AD is model-agnostic, offering flexibility, and prioritizes real-time efficiency. Thus, it seems suitable for seamless integration with industrial Decision Support Systems. We present the first industrial application of AcME-AD, showcasing its effectiveness through experiments. These tests demonstrate AcME-AD’s potential as a valuable tool for explainable AD and feature-based root cause analysis within industrial environments, paving the way for trustworthy and actionable insights in the age of Industry 5.0.

Index Terms—Anomaly Detection, Explainable Artificial Intelligence, Industrial Internet of Things, Industry 5.0, Outlier Detection, Unsupervised Learning

I. INTRODUCTION

The convergence of sensing, actuation, and communication technologies, coupled with the rise of Machine Learning (ML), has spurred the rapid development of the Internet of Things (IoT) [1]–[3]. Within this landscape, Industrial IoT (IIoT) stands out, where continuous monitoring of industrial assets is crucial for optimizing maintenance schedules and maximizing production efficiency.

Anomaly detection (AD) plays a vital role in IIoT systems, enabling the timely identification of deviations from normal behavior before they escalate into costly downtime or production issues [4]. Notably, unsupervised AD techniques are particularly advantageous in this domain, as they do not necessitate pre-labeled data, often a cumbersome and resource-intensive endeavor. However, merely identifying anomalies is insufficient. Understanding the underlying causes behind them is critical for implementing effective corrective actions. This is where explainable Artificial Intelligence (XAI) comes into play [5], [6]. XAI, also known as ML interpretability, aims to elucidate the decision-making process of ML models. While some ML methods offer inherent interpretability, others, like high-performance deep neural networks, often operate as “black boxes,” lacking

transparency in their predictions. This lack of transparency can lead to hesitation in adopting ML solutions within Decision Support Systems (DSS) due to potential trust concerns [7].

In the context of IIoT, fast and efficient XAI is critical. Rapid explanation generation is crucial for effective decision-making and prompt implementation of corrective actions, minimizing potential delays in response.

This paper examines how AcME-AD [8] an efficient, and model-agnostic approach to explainability that was recently developed, can be applied in industrial settings for AD. AcME-AD works well even with unsupervised AD, as it explains predictions by highlighting how changes in input features impact the resulting anomaly score. This, combined with its computational efficiency and effective result visualizations, makes AcME-AD ideal for industrial internet of things (IIoT) monitoring through decision support systems (DSS).

The rest of this paper is organized as follows: Section II explores the critical role of XAI in Industry 4.0 and 5.0, particularly within AD. Section III summarizes the core principles and functionalities of AcME-AD. Section IV showcases the effectiveness of AcME-AD through real-world applications in two industrial scenarios. Section V recaps key takeaways and outlines promising directions for future exploration.

II. RELATED WORK

Recent advancements in data and computational capabilities enabled the widespread adoption of ML within digital manufacturing. Transitioning towards Industry 5.0, the focus shifts to a human-centric paradigm, emphasizing collaboration between operators and intelligent systems [9]. Operators evolve from primarily executing tasks to leveraging their domain knowledge alongside AI-powered tools for informed decision-making. Consequently, the need for explainable and trustworthy predictions becomes paramount for building confidence in data-driven monitoring solutions, making ML interpretability a critical factor. Examples of explainable ML industrial solutions include fault detection in machinery [4], process monitoring in various industries

from semiconductor [10], [11] to home appliances [12], and predictive maintenance [13].

This work focuses on interpretable anomaly detection. Prior research on this topic spans diverse areas like wireless spectrum anomalies [14], robot activity recognition [15], and ICT threat detection [16]. To balance low latency with root-cause analysis insights, we leverage AcME-AD [8] to explain predictions. This approach maintains efficiency and model-agnosticism in line with AcME [17]. However, AcME-AD is uniquely tailored for (possibly unsupervised) anomaly detection (AD) tasks, assuming only that the model provides an anomaly score as output. This combination of explainability and efficiency positions AcME-AD as an ideal solution for industrial scenarios where timely and actionable insights are essential.

III. PROPOSED APPROACH

The goal of this work is to prove the effectiveness of AcME-AD [8] to explain AD models in the industrial scenario. AcME-AD offers a model-agnostic approach to explainability in AD, contrasting methods tailored for specific models like Isolation Forest [18] or for Principal Component Analysis in [19]. This flexibility allows users to leverage the best-performing AD model while gaining interpretable results from AcME-AD. Furthermore, AcME-AD prioritizes computational efficiency, making it suitable for critical scenarios requiring real-time decisions. This distinguishes it from methods like SHAP [20] which can struggle in such settings. As shown in Section IV, AcME-AD delivers explanations quickly, solidifying its value for time-sensitive applications.

Consider any AD model that produces as output an anomaly score for each data point, i.e., a scalar real value indicating its level of outlyingness, and a threshold on the anomaly score, classifying scores below the threshold as normal and above as anomalous. AcME-AD produces local explanations for a data point \mathbf{x} by systematically perturbing individual features, while keeping other features fixed, and observing the impact on the anomaly score. It utilizes a convex combination of four key metrics (all with range from 0 to 1) to compute $I_j(\mathbf{x})$, the importance of the j -feature in contributing to the anomaly score assigned to \mathbf{x} :

- 1) Delta D_j : Represents the maximum difference in anomaly scores achieved by perturbing feature j across its quantile values.
- 2) Ratio R_j : Represents the normalized distance of the original anomaly score from the minimum achievable score through j 's perturbation.
- 3) Change of Predicted Class C_j : $C_j = 1$ if feature perturbation induces a change in the classification (anomaly vs normal) of the data point \mathbf{x} , depending on the anomaly score and the threshold.
- 4) Distance to Change Q_j : Quantifies the degree of perturbation needed (in terms of quantile value) for feature j to change the classification outcome of \mathbf{x} , if possible.

Then:

$$I_j(\mathbf{x}) \doteq w_D D_j + w_C C_j + w_Q Q_j + w_R R_j$$

$$\text{s.t. } \sum_i w_i = 1, w_i \geq 0, \forall i \in \{D, C, Q, R\}.$$

The weights w_i are input parameters and can be customized. Default values are set to $w_D = 0.3, w_C = 0.3, w_R = 0.2, w_Q = 0.2$. For further details we refer to [8].

AcME-AD's *what-if* visualization tool (see for example Fig. 3) provides local explanation by exploring how the anomaly score would change if a single feature's quantile value were modified while keeping others fixed. The ten most important features, ranked by decreasing importance, are displayed. The visualization features: (i) a red dashed line representing the anomaly score of the examined data point; (ii) a black solid line indicating the normal/anomalous classification threshold; (iii) small colored bubbles, indicating the anomaly scores associated with each perturbation of the feature value and (iv) large colored bubbles on the red line depicting the data point's actual feature values. The bubble colors convey the position of the perturbed/original value within the entire dataset distribution (specifically, their quantile). By interacting with this visualization, users can understand how modifying specific feature values might impact the anomaly score and potentially transition the data point from anomalous to normal.

To identify overall important features (i.e., relevant across different anomalies), we propose the following procedure: (i) Isolate anomalies: Select all data points flagged as anomalies by the model; (ii) Localize importance: For each anomaly, employ AcME-AD to generate a local feature ranking based on importance scores; (iii) Aggregate ranks: Count how often each feature appears at each rank position across all anomalies; (iv) Visualize insights: Normalize the counts and create a stacked bar chart (see, for example Fig. 1). The x-axis represents ranking positions (1 being most important). Each bar at position k for feature j reflects the percentage of anomalies where feature j ranked k th. This allows researchers to observe which features consistently rank high across various anomalies. For many features, consider merging those ranking below 5% into an "others" category to improve readability. This threshold can be adjusted based on specific needs.

IV. EXPERIMENTAL RESULTS

This section presents the experimental results obtained using AcME-AD in two industrial scenarios. Experiments involve both a synthetic dataset and an unlabeled real-world dataset. The former provides known anomaly-causing features for initial validation, while the latter reflects real-world challenges such as high feature dimensionality and lack of supervision. The code to reproduce the experiments is available in a public repository¹.

¹<https://github.com/dandolodavid/ACME>

A. Use Case I: Chemical processes

In the first case-study, we investigate the effectiveness of AcME-AD using the Tennessee Eastman Process (TEP) dataset [21], a well-established industrial benchmark for fault and anomaly detection. This dataset, being supervised, enables us to select a high-performing AD model to explain, crucial to properly assessing our method. Since AcME-AD explains model predictions and not the underlying physical process, it is important to pick a very accurate model to leverage domain knowledge about the process for evaluation. In principle, indeed, misattributions of feature importance could be associated with shortcomings in the model rather than limitations in the interpretability approach.

TEP data are obtained by simulation using a computational model of chemical processes comprising time series originating from normal or faulty processes. Each time series contains 500 samples with 52 features. Samples are categorized into 21 classes, where Class 0 signifies normal operational states and classes 1-20 correspond to different simulated process faults. Importantly, there exists prior knowledge about the features associated with each of the first 15 faults [22], aiding the assessment of the proposed method. In our experimental setup, we consider a subset of the available dataset to reproduce an AD scenario. We randomly select 70 normal simulations and 3 faulty simulations of fault type IDV12. We select this fault type because domain knowledge about the responsible feature is available [22], [23]. Specifically, the fault IDV12 is related to the condenser cooling water input temperature, which assumes random anomalous values during the process. The true root cause feature is `xmeas_11`, which is the separator temperature measure. Among the trained models, Isolation Forest (IF) [24] is the best performing one, achieving an average precision score equal to 0.77. Results for other models can be found in the code repository.

1) *Overall feature importance*: Fig. 1 displays the overall importance bar chart for TEP. Feature `xmeas_11`, depicted in dark blue, is correctly identified as the most or second most relevant feature in a considerable percentage of anomalies, consistent with prior knowledge. It is second in importance only to `xmeas_7`, which is the reactor pressure. The authors in [22], in Section 4, build a Sign Directed Graph to model the Tennessee Eastman Process. This graph shows that reactor pressure `xmeas_7` influences `xmeas_11` through only another feature, suggesting that IF might leverage this causal relationship to detect anomalies. Consistent with prior research [8], [17], KernelSHAP [20] and AcME explanations show high similarity. This is evident when comparing Fig. 1 and 2. However, computing a local explanation with AcME-AD takes 3.03 s and with KernelSHAP 62.32 s (as detailed in Tab. Ia).

2) *Local Interpretability*: Fig. 3 illustrates AcME-AD *what-if* tool for local explanation. For this specific anomalous prediction, the feature `xmeas_11`, representing the separator temperature measurement, correctly emerges as the most relevant. Its actual value, denoted by the larger green

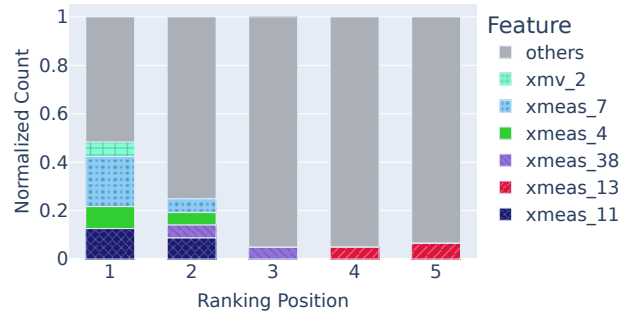


Fig. 1: AcME-AD overall importance bar chart using IF on TEP.

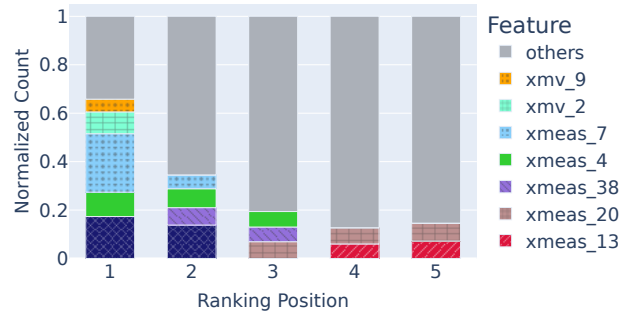


Fig. 2: KernelSHAP overall importance bar chart using IF on TEP and 10% sampling of the background dataset.

bubble, is very high with respect to the data distribution. One can notice that reducing the separator temperature would transition the point to a normal state, at least up to a certain quantile value, represented by the leftmost light blue point. After that, further decreases in the separator temperature would classify the data point as abnormal again. The only other feature that, if perturbed, would induce a change of state is `xmv_9`, representing the stripper steam valve, a manipulated process variable. The pattern exhibited by this feature closely resembles that of `xmeas_11`.

B. Use Case II: Packaging equipment

The second industrial case-study considers the monitoring of packaging machines. The experiments are conducted on the publicly available² Packaging Industry Anomaly DEtection (PIADE) dataset [25], which contains unlabeled data acquired by five industrial packaging machines. We consider sequences data, where raw observations are aggregated considering 1-hour-long time windows. Because the five machines have different operating points, in this paper, we present results obtained considering the second machine with `Equipment_ID` equal to 2. Results for other machines can be found in the repository. The dataset contains 2725 data points characterized by 162 features.

1) *Model selection with AcME-AD*: In IIoT datasets, such as in PIADe, labels are often not available. Typically, practitioners resort to ensembles of AD models. When one of the models detects an anomalous data point, an alarm

²<https://zenodo.org/records/7071747>

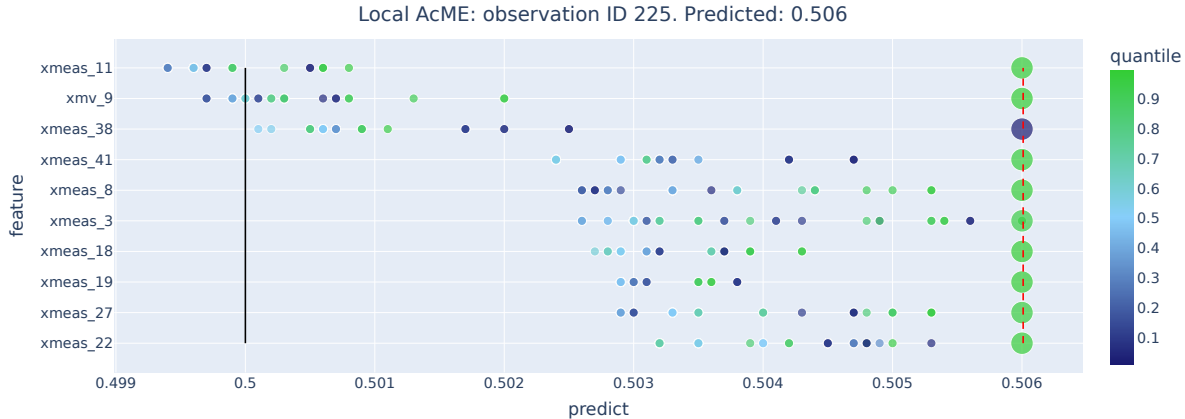


Fig. 3: AcME-AD Local explanation of an anomaly identified by IF in TEP. It emerges that this data point would be considered normal by modifying the values of `xmeas_11` or `xmv_9`.

is triggered. However, this approach often generates a considerable number of false positives. Instead, AcME-AD can be exploited to select a suitable AD model. This selection process is informed by the features identified as relevant for each model according to AcME-AD. This opportunity is strictly related to the model-agnostic nature of AcME-AD.

We compute the overall importance for a set of candidate AD models as detailed in Section III. Then, in collaboration with subject matter experts, it is possible to select Lightweight on-line detector of anomalies (LODA) [26] as the model that best aligns with their domain knowledge about the underlying process. Fig. 5 shows the resulting overall importance visualization. As expected by the domain experts, the most relevant features are the count of alarms `count_sum` and the number of state changes `#changes`, followed by specific alarms such as `A_017` and `A_010` that are related to known failures, and `downtime/downtime` that is related to persistent downtime status.

2) *Local Interpretability*: As a demonstrative example, let’s consider a randomly sampled data point detected as anomalous by LODA. We generate the corresponding AcME-AD’s *what-if* visualization, displayed in Fig. 4. There are four features that, if perturbed, would bring the data point to a normal state. Among these, the most important is `count_sum`. We recall that this feature counts the number of alarms occurred within the 1-hour interval described by the data point. Its original value, represented by the larger green bubble, falls within the highest quantile of the training set. The other smaller bubbles show the anomaly scores resulting from perturbations of `count_sum` across various quantiles, while keeping the other features fixed. As the `count_sum` value decreases, depicted by the gradual change in color of the bubbles from green to blue, the data point tends toward normality. This behavior aligns with domain knowledge, where a high number of alarms typically indicates issues in the machine, thus being anomalous situations. Notably, even a slight pertur-

bation of `count_sum` leads to the classification of the data point as normal. The second most relevant feature is `downtime/downtime`. The anomaly score behavior closely mirrors that of `count_sum`. This 1-hour-sequence data point exhibits a high frequency of transitions from downtime to downtime, which is indeed atypical. The third feature which perturbation can induce a classification change is `A_012`. Many occurrences of this process alarm are associated with high production levels in the equipment under consideration. Consequently, frequent occurrences of this alarm can be interpreted as an indication of a normal and desirable operational situation. The current value of `A_012` has a light blue color, suggesting a significantly reduced machine throughput compared to the majority of all the data points. The *what-if* tool points out that if the number of `A_012` increases (the green bubble), the data point would return to a normal classification, which is aligned with domain expertise. The last feature that can be perturbed to normalize the sequence is `idle/performance_loss`, which counts the number of machine transitions from idle to a performance loss state within the interval. However, the absence of a correlation between the values assumed by this feature and the corresponding anomaly score suggests that the feature can not be effectively utilized for taking corrective actions.

This analysis demonstrates how AcME-AD empowers users to pinpoint feature-specific interventions that can potentially bring anomalous data points back to normal, aiding in informed decision-making and system restoration.

C. AcME-AD and KernelSHAP: time comparison

The *de-facto* standard model-agnostic method for explaining models, including unsupervised AD ones, is KernelSHAP [20]. Despite its solid theoretical foundation, the computational overhead of KernelSHAP is a recognized issue [17]. Specifically, the computational time quickly escalates with the size of the dataset used to fit the ex-

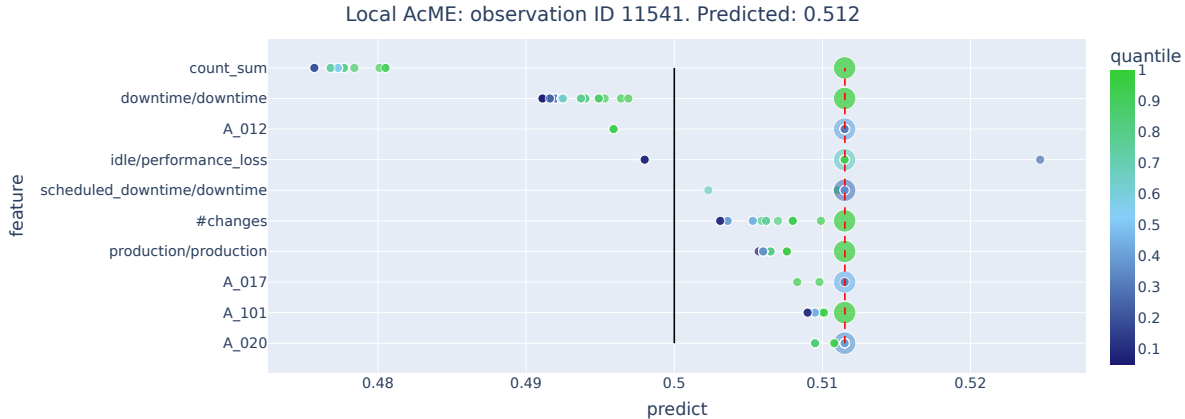


Fig. 4: AcME-AD Local explanation of a randomly sampled anomaly identified by LODA in PIADe.

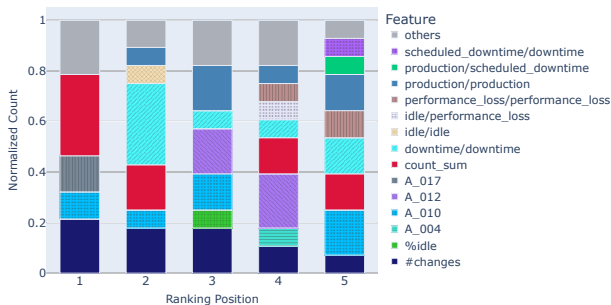


Fig. 5: Overall importance bar chart for LODA on PIADe sequences - Equipment 2.

plainer, denoted as *background*, which is typically equal to the training set. The authors in [27] propose to reduce the size of the background by randomly sub-sampling the original dataset. However, as extensively demonstrated in [17], this operation may lead to unreliable explanations, especially in complex dataset distributions. Table Ia reports the time³ required to compute a local explanation of a single anomalous data point using AcME-AD and KernelSHAP on TEP. Due to limited resources, we were able to compute only the time of KernelSHAP using at most half of the training set as background. Our findings reveal that AcME-AD is an order of magnitude faster than KernelSHAP even when using the 5% as background. When utilizing the 20% and the 50% sampling, the time demand makes KernelSHAP incompatible with the integration in Decision Support Systems.

Table Ib illustrates the elapsed time when analyzing PIADe data. In this case, the gap is less pronounced. The motivation behind this lies in the fact that, for the same number of features, the time complexity of KernelSHAP

³For reference, experiments are conducted on AMD Ryzen 7 3700X, 3.6GHz, RAM 20GB.

	Background Size	Elapsed time IF (s)
AcME-AD	36500 (100%)	3.03
KernelSHAP	1825 (5%)	30.23
KernelSHAP	3650 (10%)	62.32
KernelSHAP	7300 (20%)	123.75
KernelSHAP	36500 (50%)	655.64

(a) TEP dataset.

	Background Size	Elapsed time LODA (s)
AcME-AD	2725 (100%)	18.63
KernelSHAP	681 (25%)	16.46
KernelSHAP	1362 (50%)	33.21
KernelSHAP	2043 (75%)	49.58
KernelSHAP	2725 (100%)	65.64

(b) PIADe dataset

TABLE I: Single explanation times for AcME-AD and KernelSHAP.

is dominated by the number of data points, whereas the complexity of AcME-AD is driven by the dimensionality of the samples (i.e., the number of features). PIADe has a high number of features (162) and a low number of samples (2725) when compared to TEP (36500). Nevertheless, once again, AcME-AD generally outperforms KernelSHAP in terms of speed, achieving comparable performance only for 25% sampling. Moreover, this discrepancy becomes substantial when exploiting the explainability method for model selection, as in Section IV-B1, where local explanations need to be generated for every predicted anomalous point.

Finally, it is noteworthy that there exist model-specific variants of SHAP which, by leveraging the specific structure of the models, demand lower computational time. However, in this comparison, we solely focus on KernelSHAP to ensure a fair evaluation of AcME-AD, which is model-agnostic.

V. CONCLUSIONS

This work successfully demonstrates the application of our proposed method, AcME-AD, for anomaly detection in an industrial setting. Firstly, AcME-AD facilitates user decision-making through clear and informative visualizations. The integrated "what-if" tool for local interpretation empowers users to pinpoint the root cause of anomalies and take appropriate corrective actions. Secondly, its efficient computation enables seamless integration into decision support systems, promoting real-time anomaly detection and response. We highlight the particular suitability of AcME-AD for unsupervised anomaly detection tasks, which are of paramount importance in industrial applications. By providing model-agnostic explanations, AcME-AD empowers domain experts to select models that best align with their knowledge, fostering crucial human-machine collaboration in the context of Industry 5.0. As future development of the present work, we aim at refining the visualizations based on feedback from real-world deployments. Additionally, we plan to explore the potential of utilizing local explanations for clustering anomalies into distinct groups, thereby enabling supervised classification tasks.

ACKNOWLEDGMENTS

This work was partially carried out within the MICS (Made in Italy – Circular and Sustainable) Extended Partnership and received funding from Next-GenerationEU (Italian PNRR – M4C2, Invest 1.3 – D.D. 1551.11-10-2022, PE00000004). Moreover this study was also partially carried out within the PNRR research activities of the consortium iNEST (Interconnected North-Est Innovation Ecosystem) funded by the European Union Next-GenerationEU (Piano Nazionale di Ripresa e Resilienza (PNRR) – Missione 4 Componente 2, Investimento 1.5 – D.D. 1058 23/06/2022, ECS00000043). This work was also cofunded by the European Union in the context of the Horizon Europe project 'AIMS5.0 - Artificial Intelligence in Manufacturing leading to Sustainability and Industry5.0' Grant agreement ID: 101112089.

REFERENCES

- [1] N. Bargellesi, A. Beghi, M. Rampazzo, and G. A. Susto, "Autoss: A deep learning-based soft sensor for handling time-series input data," *IEEE Robotics and Automation Letters*, vol. 6, no. 3, pp. 6100–6107, 2021.
- [2] T. J. Saleem and M. A. Chishti, "Deep learning for the internet of things: Potential benefits and use-cases," *Digital Communications and Networks*, vol. 7, no. 4, pp. 526–542, 2021.
- [3] Z. Kang, C. Catal, and B. Tekinerdogan, "Machine learning applications in production lines: A systematic literature review," *Computers & Industrial Engineering*, vol. 149, p. 106773, 2020.
- [4] L. C. Brito, G. A. Susto, J. N. Brito, and M. A. Duarte, "An explainable artificial intelligence approach for unsupervised fault detection and diagnosis in rotating machinery," *Mechanical Systems and Signal Processing*, vol. 163, p. 108105, 2022.
- [5] L. H. Gilpin, D. Bau, B. Z. Yuan, A. Bajwa, M. Specter, and L. Kagal, "Explaining explanations: An overview of interpretability of machine learning," in *2018 IEEE 5th International Conference on Data Science and Advanced Analytics (DSAA)*, 2018, pp. 80–89.
- [6] A. Adadi and M. Berrada, "Peeking inside the black-box: A survey on explainable artificial intelligence (xai)," *IEEE Access*, vol. 6, pp. 52 138–52 160, 2018.
- [7] C. Nicodeme, "Build confidence and acceptance of ai-based decision support systems - explainable and liable ai;" in *2020 13th International Conference on Human System Interaction (HSI)*, 2020, pp. 20–23.
- [8] V. Zaccaria, D. Dandolo, C. Masiero, and G. A. Susto, "Acme-ad: Accelerated model explanations for anomaly detection," 2024. [Online]. Available: <https://arxiv.org/abs/2403.01245>
- [9] I. Ahmed, G. Jeon, and F. Piccialli, "From artificial intelligence to explainable artificial intelligence in industry 4.0: A survey on what, how, and where," *IEEE Transactions on Industrial Informatics*, vol. 18, pp. 5031–5042, 2022. [Online]. Available: <https://api.semanticscholar.org/CorpusID:246366040>
- [10] M. Carletti, M. Maggipinto, A. Beghi, G. A. Susto, N. Gentner, Y. Yang, and A. Kyek, "Interpretable anomaly detection for knowledge discovery in semiconductor manufacturing," in *2020 Winter Simulation Conference (WSC)*. IEEE, 2020, pp. 1875–1885.
- [11] B. Feng, S.-B. Kim, S. Lazarova-Molnar, Z. Zheng, T. Roeder, and R. M. Thiesing, "Interpretable anomaly detection for knowledge discovery in semiconductor manufacturing," 2020.
- [12] M. Carletti, C. Masiero, A. Beghi, and G. A. Susto, "A deep learning approach for anomaly detection with industrial time series data: a refrigerators manufacturing case study," *Procedia Manufacturing*, vol. 38, pp. 233–240, 2019.
- [13] S. Vollert, M. Atzmueller, and A. Theissler, "Interpretable machine learning: A brief survey from the predictive maintenance perspective," in *2021 26th IEEE International Conference on Emerging Technologies and Factory Automation (ETFA)*, 2021, pp. 01–08.
- [14] S. Rajendran, W. Meert, V. Lenders, and S. Pollin, "Unsupervised wireless spectrum anomaly detection with interpretable features," *IEEE Transactions on Cognitive Communications and Networking*, vol. 5, no. 3, pp. 637–647, 2019.
- [15] B. Hayes and J. A. Shah, "Interpretable models for fast activity recognition and anomaly explanation during collaborative robotics tasks," in *2017 IEEE International Conference on Robotics and Automation (ICRA)*, 2017, pp. 6586–6593.
- [16] R. Orizio, S. Vuppala, S. Basagiannis, and G. Provan, "Towards an explainable approach for insider threat detection: Constraint network learning," in *2020 International Conference on Intelligent Data Science Technologies and Applications (IDSTA)*, 2020, pp. 42–49.
- [17] D. Dandolo, C. Masiero, M. Carletti, D. Dalle Pezze, and G. A. Susto, "Acme—accelerated model-agnostic explanations: Fast whitening of the machine-learning black box," *Expert Systems with Applications*, vol. 214, p. 119115, 2023.
- [18] M. Carletti, M. Terzi, and G. A. Susto, "Interpretable anomaly detection with diffi: Depth-based feature importance of isolation forest," *Engineering Applications of Artificial Intelligence*, vol. 119, p. 105730, 2023.
- [19] N. Takeishi, "Shapley values of reconstruction errors of pca for explaining anomaly detection," in *2019 international conference on data mining workshops (icdmw)*. IEEE, 2019, pp. 793–798.
- [20] S. M. Lundberg and S.-I. Lee, "A unified approach to interpreting model predictions," *Advances in neural information processing systems*, vol. 30, 2017.
- [21] C. A. Rieth, B. D. Amsel, R. Tran, and M. B. Cook, "Additional tennessee eastman process simulation data for anomaly detection evaluation," *Harvard Dataverse*, vol. 1, p. 2017, 2017.
- [22] M. G. Don and F. Khan, "Dynamic process fault detection and diagnosis based on a combined approach of hidden markov and bayesian network model," *Chemical Engineering Science*, vol. 201, pp. 82–96, 2019.
- [23] R. R. A. Harinarayan and S. M. Shalinie, "Xfddc: explainable fault detection diagnosis and correction framework for chemical process systems," *Process Safety and Environmental Protection*, vol. 165, pp. 463–474, 2022.
- [24] F. T. Liu, K. M. Ting, and Z.-H. Zhou, "Isolation forest," in *2008 eighth ieee international conference on data mining*. IEEE, 2008, pp. 413–422.
- [25] T. Diego, C. Enrico, C. Masiero, G. Susto, A. Beghi *et al.*, "Packaging industry anomaly detection (piade) dataset," 2022.
- [26] T. Pevný, "Loda: Lightweight on-line detector of anomalies," *Machine Learning*, vol. 102, pp. 275–304, 2016.
- [27] S. Lundberg, "Shap api - online documentation," 2020. [Online; accessed 08-January-2024]. [Online]. Available: <https://shap.readthedocs.io/en/latest/generated/shap.KernelExplainer.html#shap.KernelExplainer>